Synthesis and Structure of Monomeric and Platinum-Bonded (1,10-Phenanthroline)thallium Complexes

Guibin Ma,*[b] Andreas Fischer,[a] and Julius Glaser*[a]

Keywords: Metal−metal interactions / Platinum / Thallium / N ligands / NMR spectroscopy

Oxidative addition of (1,10-phenanthroline)thallium(III) complexes $[Tl(phen)_n(solv)]^{3+}$ (n = 1–2) (phen = 1,10-phenanthroline) to $[Pt(CN)_4]^{2-}$ in DMSO, in the presence of cyanide ions and in the absence of cyanide ions yielded heterodinuclear metal–metal-bonded complexes, $[(NC)_5Pt–Tl(phen)_n(solv)]$ and $[(NC)_4Pt–Tl(phen)_n(solv)]^+$ (n = 0, 1, and 2), respectively. The presence of a direct Pt–Tl bond in the complex is evident by a very strong one-bond $^{195}Pt–^{205}Tl$ spin-spin coupling detected by ^{205}Tl NMR: ^1J = 94.0 kHz (**1a**), 84.2 kHz (**2a**), and 77.1 kHz (**3a**) corresponding to n = 0, 1, and 2 in $[(NC)_4Pt–Tl(phen)_n(solv)]^+$, and ^1J = 65.4 kHz (**2b**) and 62.5 kHz (**3b**) for n = 1 and 2, respectively, in $[(NC)_5Pt–Tl(phen)_n(solv)]$. The crystal structures of $[(NC)_5Pt–Tl(phen)(DMSO)_3]\cdot(DMSO)$ (**2b**), $[(NC)_5Pt–Tl(phen)_2]\cdot(DMSO)_3$ (**3b**), and $[Tl(phen)_2Cl_2](ClO_4)$ (**4**) complexes were determined. Very short Pt–Tl bonds, 2.6296(3) and 2.6375(5) Å, are present in structures **2b** and **3b**, respectively. The corresponding force constants in the molecules in the solid state, 1.84 and 1.74 N/cm for **2b** and **3b**, respectively, were calculated using Raman stretching frequencies of the Pt–Tl vibrations, and are characteristic for a single, strong metal–metal bond. Electronic absorption spectra were recorded for selected compounds and the optical transition attributed to the metal–metal bond was assigned.

Introduction

Square-planar complexes of d^8 transition metal ions comply with the 16-electron rule, the occupied d_{z^2} orbital can act as a potential donor to another metal ion (M), resulting in a dative $M(d^8)\rightarrow M$ bond. Many $Pt^{II}-M$ dative-bond complexes have been reported.[1a] A direct metal−metal bond between platinum(II) and thallium(I) in the solid state was first described by Nagle et al.[1b] Recently, several compounds containing a Pt−Tl bond have been prepared.[2] In this laboratory, a family of four dinuclear platinum−thallium cyano compounds with the formula $[(NC)_5Pt-Tl(CN)_{n-1}(aq)]^{(1-n)}$ (n = 1−4 for compound **I**, **II**, **III** and **IV**, respectively), which contain a direct metal−metal bond unsupported by ligands, have been synthesized and characterized in aqueous solutions.[3] Due to the light sensitivity of the Pt−Tl metal−metal bond in these compounds, they are of principal interest. A study was initiated of the effects of modifications of these compounds with nitrogen donor and chromophore organic ligands, e.g. 2,2′-bipyridine and porphyrin (tpp, thpp).[4] When the compounds were exposed to daylight, two-electron transfer was induced between the metal ions. Thus, possible applications in photovoltaic devices, for example in a "wet" solar cell of Grätzel-type,[5] can be envisaged. In the search for suitable compounds for future applications, we report here the synthesis and structural characteristics of new complexes containing a direct metal−metal bond, $[(NC)_4Pt-Tl(phen)_n(solv)]^+$ with n = 0 (**1a**), 1 (**2a**), 2 (**3a**) and $[(NC)_5Pt-Tl(phen)_n(solv)]$ with n = 1 (**2b**), 2 (**3b**). For the first time, a naked Pt−Tl bond with the formal oxidation states Pt^{II} and Tl^{III} and the composition $[(NC)_4Pt-TlX]^+$ was synthesised and structurally characterised [X = $(phen)_n(solv)$, n = 0,1,2; solv = DMSO].

Results and Discussion

Characterization in Solution by ^{205}Tl NMR Spectroscopy

The preparation of Pt−Tl complexes with the N-donor ligand ethylenediamine was described in our previous paper.[4a] In a similar way, two new Pt−Tl complexes $[(NC)_4Pt-Tl(solv)]^+$ (**1a**) and $[(NC)_5Pt-Tl(solv)]$ (**1b**) could be prepared; these two species were then treated with 1,10-phenanthroline, whereby the complexes $[(NC)_4Pt-Tl(phen)(solv)]^+$ (**2a**), $[(NC)_5Pt-Tl(phen)(solv)]$ (**2b**), $[(NC)_4Pt-Tl(phen)_2(solv)]$ (**3a**), and $[(NC)_5Pt-Tl(phen)_2]$ (**3b**) in DMSO solution (Scheme 1) were prepared.

In the reaction between the solid compound $[Tl(DMSO)_6](ClO_4)_3$ and $[Pt(CN)_4{}^{2-}]$ in DMSO (cf. Scheme 1, lower part), it is clear from the ^{205}Tl NMR spectrum that only

[a] Department of Chemistry, Royal Institute of Technology (KTH)
10044 Stockholm, Sweden
E-mail: julius@inorg.kth.se
[b] Department of Chemistry, Shanxi University,
030006 Taiyuan, Shanxi Province, P. R. China
Supporting information for this article is available on the WWW under http://www.eurjic.com or from the author.

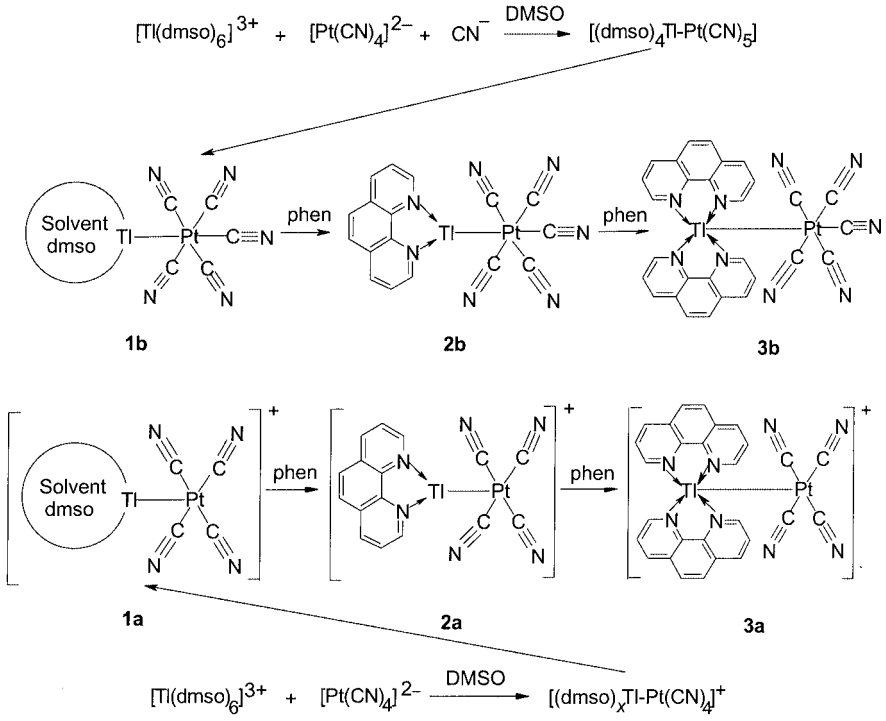

Scheme 1

one Pt−Tl dinuclear complex forms (**1a**); a 1:3.9:1 triplet peak appears centred at δ = 82 with a large spin-spin coupling constant (94000 Hz), this is characteristic for a non-buttressed Pt−Tl bond.[3] The ^{205}Tl NMR signal splits into a doublet by nuclear spin-spin coupling to the NMR-active isotope ^{195}Pt (natural abundance 33.8%, I = 1/2) and, together with the NMR-inactive Pt isotopes (natural abundance 66.2%), it shows a triplet pattern with the expected intensity ratio 1:3.9:1 (cf. Figure 1). Then, upon stepwise addition of 1,10-phenanthroline, two Pt−Tl species showed up in the spectra as typical triplet signals at δ = 472 (**2a**) and δ = 775 (**3a**) with the spin-spin coupling constants 84200 Hz and 77120 Hz, respectively.

The preparation and characterization of [(NC)$_5$Pt−Tl(solv)] (**1b**) was studied earlier[4a] and crystalline [(NC)$_5$Pt−Tl(DMSO)$_4$] was obtained. When the solid [(NC)$_5$Pt−Tl(DMSO)$_4$] was treated with 1,10-phenanthroline at different molar ratios (cf. Scheme 1, top part), it dissolved completely, and the complexes [(NC)$_5$Pt−Tl(phen)$_n$] (n = 1−2 for compounds **2b** and **3b**, respectively) formed in solution. The ^{205}Tl NMR chemical shifts for the two new phenanthroline species are δ = 992 and 1162, and spin-spin coupling constants ^1J(^{195}Pt-^{205}Tl) are 65440 and 62490 Hz for **2b** and **3b** in DMSO, respectively. Similar to the ^{205}Tl NMR spectrum discussed above, the signals are triplets with the expected intensity ratio 1:3.9:1 (Figure 2).

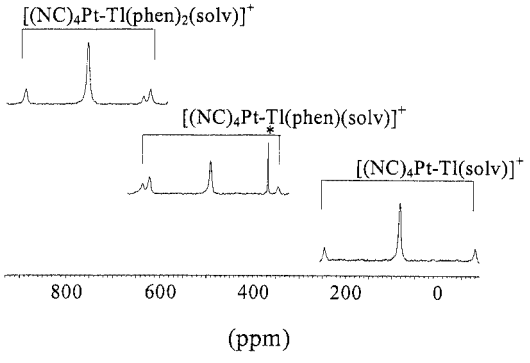

Figure 1. 288 MHz ^{205}Tl NMR spectra of Pt−Tl compounds in DMSO: [(NC)$_4$Pt−Tl(solv)]$^+$ (**1a**), [(NC)$_4$Pt−Tl(phen)(solv)]$^+$ (**2a**), and [(NC)$_4$Pt−Tl(phen)$_2$(solv)]$^+$ (**3a**); * represents Tl^I signal at δ = 363

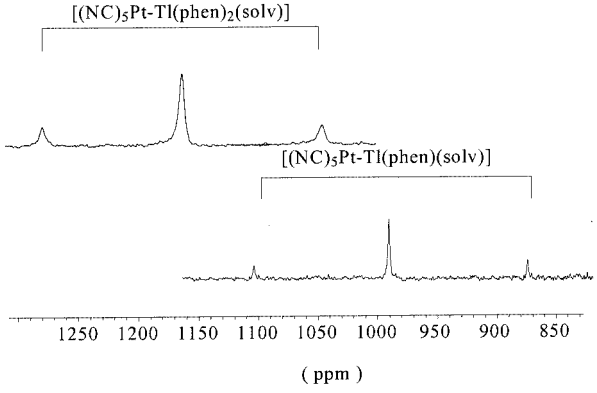

Figure 2. 288 MHz ^{205}Tl NMR spectra of the Pt−Tl compounds [(NC)$_5$Pt−Tl(phen)(DMSO)$_y$] (**2b**) and [(NC)$_5$Pt−Tl(phen)$_2$] (**3b**) in DMSO

The large spin-spin coupling constants show that a Pt−Tl bond is formed; the appearance of peaks with different and hitherto unreported chemical shifts and coupling constants suggests that new complexes $[(NC)_4Pt-Tl(phen)_n]^+$ (n = 1 and 2 for **2a** and **3a**, respectively) and $[(NC)_5Pt-Tl(phen)_n]$ (n = 1 and 2 for **2b** and **3b**, respectively) formed in solution (Scheme 1). Upon coordination of the second phen molecule to the thallium atom in all the studied Pt−Tl dinuclear complexes in DMSO, the spin-spin coupling constant $^1J(^{195}Pt\text{-}^{205}Tl)$ decreased. This strong coupling is a characteristic feature of the bonding between the two metal ions with the formal oxidation states $Pt^{II}-Tl^{III}$, and is an indication of a significant contribution of thallium 6s orbitals to the metal−metal bonding.[3b] Owing to the relativistic effects, the thallium 6s orbital is stabilized and contracted; this results in an increased electron density at the nucleus, which contributes to the Fermi contact term for spin-spin coupling.[2j,23] It was found that there is a correlation between the spin-spin coupling constant and the metal−metal separation/bond strength in the series of complexes $[(NC)_5Pt-Tl(CN)_n]^{n-}$ (n = 1−3). The stronger Pt−Tl bonding, the shorter Pt−Tl bond length and the larger spin-spin coupling constant.[6]

NMR chemical shifts for heavy metals with large chemical shift ranges are very sensitive to the oxidation state of the metal ion.[7] Thus, ^{205}Tl NMR chemical shifts of Tl^I species are in the range δ = −200 to +200 and those of Tl^{III} complexes are usually at δ = 2000 to 3000.[3d] In DMSO, ^{205}Tl NMR chemical shifts of $[Tl(DMSO)_6]^{3+}$ and Tl^+ are δ = 1886 and 361, respectively.[11] For the currently studied compounds, $[(NC)_4Pt-Tl(solv)]^+$, $[(NC)_4Pt-Tl(phen)_n]^+$ (n = 1−2), and $[(NC)_5Pt-Tl(phen)_n]$ (n = 1−2), ^{205}Tl NMR chemical shifts are in the Tl^+ region for $[(NC)_4Pt-Tl(solv)]^+$ and between Tl^I and Tl^{III} for all the others. Consequently, the thallium oxidation state in these compounds is between Tl^I and Tl^{III}.[6a] It could be of interest to compare the differences between the spin-spin coupling constants $^1J(^{195}Pt\text{-}^{205}Tl)$ for the two types of complexes prepared in this work in which the only difference between the compounds **a** and **b** is one extra cyanide ligand bound to the platinum atom. Still, the differences in coupling constants are very large: 28100 Hz [between ^1J(**1a**) and ^1J(**1b**)], 18800 Hz [between ^1J(**2a**) and ^1J(**2b**)], and 15600 Hz [between ^1J(**3a**) and ^1J(**3b**)].

Crystal Structures of Pt-Bonded and Monomeric Tl(phen) Compounds

$[(NC)_5Pt-Tl(phen)(DMSO)_3]$ (DMSO) (2b)

Single crystals of the dinuclear compound **2b** were obtained from the studied solution and the structure determined by X-ray diffraction method. The ORTEP perspective view of the molecular structure and the selected bond lengths of **2b** are shown in Figure 3. The Pt−Tl bond length is short, 2.6296(3) Å, significantly shorter than for other reported Pt−Tl bond lengths.[2] In the $Pt(CN)_5$ moiety the Pt−C bonds range between 2.005 and 2.053 Å; the axial cyanide has a slightly longer Pt−C distance than the equatorial ones. The Tl atom coordinates one phen ligand and three DMSO molecules forming a distorted octahedral geometry around the thallium atom. Atoms O1, O4, O5, and N2 define an equatorial plane, from which the Tl atom is displaced 0.57(1) Å towards the Pt atom. The four equatorial ligand atoms around Tl are in a staggered conformation to the adjacent square-planar $Pt(CN)_4$ unit. The angle between the Tl1−N1 bond and the plane formed by the atoms O1, O4, and O5 is 91.6°, close to perpendicular, whereas the angle N1−Tl1−Pt1 is 176.1°, close to 180°. In this compound, two kinds of DMSO molecules are present in the structure; three molecules coordinated to the thallium atom and one remains uncoordinated. The bond lengths of the coordinated DMSO molecules are altered compared to the uncoordinated one. The strong coordination gives a short Tl−O and a long S−O bond length [for coordinated DMSO: Tl1−O1 = 2.448(4) Å, S2−O1 = 1.527(5) Å; Tl1−O4 = 2.471(4) Å, S1−O4 = 1.511(5) Å; Tl1−O5 = 2.495(5) Å, S4−O5 = 1.499(6) Å; for free DMSO: S3−O6 = 1.483(8) Å]. The S−O bond order is diminished by coordination, and it is due to electrons of the oxygen atom moving toward the thallium atom upon coordination. Comparing these data to our previous structural data of $[Tl(DMSO)_6]^{3+}$ [Tl−O = 2.224(3) Å, S−O = 1.544(4) Å],[11] the Tl−DMSO coordination is much weaker in compound **2b**. It is probably due to the decreased positive charge of thallium in the dinuclear complex.

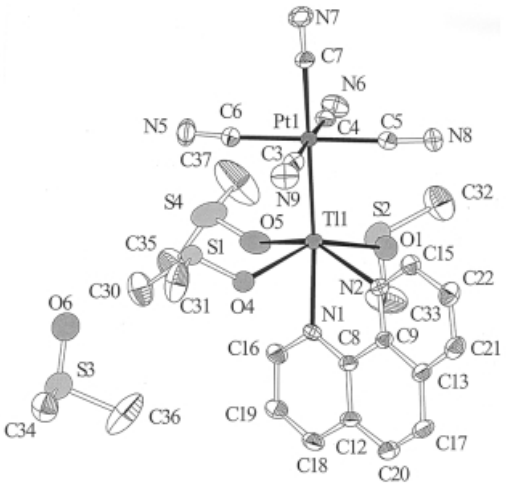

Figure 3. ORTEP view of the species $[(NC)_5Pt-Tl(phen)(DMSO)_3]$ found in the crystal structure of $[(NC)_5Pt-Tl(phen)(DMSO)_3]\cdot(DMSO)$ (**2b**), thermal ellipsoids are drawn at 30% probability level; selected bond lengths [Å] and angles [°]: Pt(1)−Tl(1) 2.6296(3), Pt(1)−C(3) 2.030(6), Pt(1)−C(4) 2.007(6), Pt(1)−C(5) 2.011(6), Pt(1)−C(6) 2.005(6), Pt(1)−C(7) 2.053(6), Tl(1)−N(1) 2.322(4), Tl(1)−N(2) 2.434(4), Tl(1)−O(1) 2.448(4), Tl(1)−O(4) 2.471(4), Tl(1)−O(5) 2.495(5), S(1)−O(4) 1.511(5), S(2)−O(1) 1.527(5), S(4)−O(5) 1.499(6); C(6)−Pt(1)−C(5) 177.4(2), C(3)−Pt(1)−C(4) 177.4(2), C(7)−Pt(1)−Tl(1) 177.58(18), N(1)−Tl(1)−Pt(1) 176.21(12)

$[(NC)_5Pt-Tl(phen)_2]$ 3(DMSO) (3b)

The ORTEP perspective view of the molecular structure and the selected bond lengths of **3b** are shown in Figure 4. Similar to compound **2b**, the main structural feature of **3b**

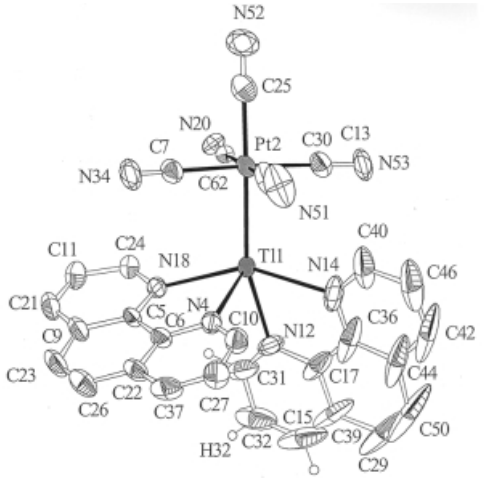

Figure 4. ORTEP view of the species $[(NC)_5Pt-Tl(phen)_2]$ found in the crystal structure of $[(NC)_5Pt-Tl(phen)_2]\cdot(3dmso)$ (**3b**); thermal ellipsoids are drawn at 30% probability level; selected bond lengths [Å] and angles [°]: Pt(1)−Tl(1) 2.6375(5), Pt(2)−C(7) 2.029(10), Pt(2)−C(13) 2.022(11), Pt(2)−C(25) 2.025(14), Pt(2)−C(30) 2.002(14), Pt(2)−C(62) 1.990(9), Tl(1)−N(4) 2.428(7), Tl(1)−N(12) 2.291(10), Tl(1)−N(14) 2.524(10), Tl(1)−N(18) 2.445(7); C(25)−Pt(2)−Tl(1) 178.3(4), N(4)−Tl(1)−Pt(2) 118.2(2), N(14)−Tl(1)−Pt(2) 103.1(4), N(18)−Tl(1)−Pt(2) 103.55(17), N(12)−Tl(1)−Pt(2) 158.6(2), C(30)−Pt(2)−C(13) 90.8(5), C(13)−Pt(2)−C(7) 177.6(4)

is the short and non-buttressed Pt−Tl bond [Pt−Tl = 2.6375(5) Å]. In addition to the Pt−Tl linkage, the platinum atom of **3b** is bonded to five carbon atoms of the cyanide ligands. Four carbon atoms constitute an almost square plane around the platinum atom, while the fifth carbon atom occupies an axial position in the pseudo-octahedron. The Tl atom is linked to four N atoms (two phen molecules), which together with the bond to Pt form irregular five-coordinated surroundings (Figure 4). The two coordination planes of the phenanthroline ligands around Tl are skewed relative to each other (torsion angle 60.8°), reminding one of butterfly wings. All carbon atoms located in the phenanthroline planes including N12 and N14 exhibit very large atomic displacement parameters; this is probably due to the relatively large free space around them.

The main structural feature of these dimetallic compounds is the short and unsupported Pt−Tl bond with the bond lengths 2.6296(3) and 2.6375(5) Å in **2b** and **3b**, respectively. These Pt−Tl distances fall into the range of values obtained previously in this laboratory for the family of related compounds: $[(NC)_5Pt-Tl(CN)_n(H_2O)_m]^{3-n}$ (n = 0−3; 2.598−2.638 Å),[6] $[(NC)_5Pt-Tl(DMSO)_4]$ (2.6131 Å),[4] $[(NC)_5Pt-Tl(en)_2]$ (2.6348 Å),[4] and $[(NC)_5Pt-Tl(bipy)_n]$ [n = 1−2; 2.6186(8) Å and 2.6117(5) Å, respectively]. The bond lengths of the hitherto characterized Pt−Tl compounds are related to the formal oxidation states of the metal ions $[Pt^0-Tl^I]$ (2.860−3.047 Å);[2a,2b] $Pt^{II}-Tl^I$ (2.876−3.152 Å);[1,2f−2i] $Pt^{II}-Tl^{II}$ (2.698−2.708);[2c,2d] and $Pt^{II}-Tl^{III}$ (2.598−2.638 Å) (refs.[3,4] and present work) Considering only the compounds of divalent platinum, it appears that the Pt−Tl bond becomes shorter when the formal oxidation state of thallium increases from Tl^I to Tl^{III}. This is consistent with both the decreasing size of the thallium cation and with the strengthening of the metal−metal interaction due to participation of the thallium 6s orbitals in the bonding.[3]

Raman vibration bands for the crystalline compounds $[(NC)_5Pt-Tl(phen)(DMSO)_3]$ and $[(NC)_5Pt-Tl(phen)_2]\cdot(DMSO)_3$ were detected at 177 and 172 cm^{-1}, respectively. The Pt−Tl force constants in the title molecules, 1.84 and 1.74 N/cm for **2b** and **3b**, were estimated using the diatomic oscillator approximation model.[8,9] These values are larger than those of the previously studied Pt−Tl cyano complexes (about 1.6 N/cm for the diatomic approximation).[3b,6] It shows that the phenanthroline ligand coordination stabilizes the Pt−Tl metal−metal bonding. The relation between the force constant and the Pt−Tl bond length was observed in the previously studied compounds $[(NC)_5Pt-Tl(CN)_n]^{n-}$ (n = 1−3) [the bond lengths are 2.598(3), 2.618(4), and 2.638(4) Å, which corresponds to force constants of 1.736, 1.693, and 1.563 N/cm, respectively).[6] A correlation seems to exist between the force constant and the Pt−Tl bond length within this series of compounds. In the present case, the ligand coordinated to the thallium atom is different, so the results are not expected to fit into the series of cyano compounds. A similar trend is, however, observed in **2b** and **3b**; the bond lengths are 2.6296(3) and 2.6375(5) Å, and the corresponding force constants are 1.85 and 1.74 N/cm, respectively. Even if the force constants increase when the cyano ligands are replaced by phenanthroline in the Tl sphere of the dinuclear Pt−Tl complex, the constants are still compatible with a single metal−metal bond.[10] The C≡N stretching region of the dinuclear species is also informative and can provide an additional support for the structure of the compounds. We assigned the two sharp bands at $\tilde{\nu}$ = 2174 and 2161 cm^{-1} for **2b** and at 2178 and 2160 cm^{-1} for **3b** to the symmetric (A_{1g}) and antisymmetric (B_{1g}) stretching vibrations of the four equivalent cyanide ligands of the $Pt(CN)_4$ unit in D_{4h} symmetry.[18] These bands shift to high frequency and are very close to the stretching bands at 2153 cm^{-1} (s) and 2137 cm^{-1}(m) for $[Pt(CN)_4]^{2-}$ in the solid state. The higher frequency bands at 2184 cm^{-1} and 2189 cm^{-1} were assigned to the axial cyanide in compounds **2b** and **3b**, respectively.

$[Tl(phen)_2Cl_2](ClO_4)$ (4)

The molecular structure of the cation $[Tl(phen)_2Cl_2]^+$ is shown in Figure 5. The thallium atom is six-coordinated and is bonded to four nitrogen atoms of two 1,10-phenanthroline ligands and to two chloride ions. Interestingly, the two phen planes are almost perpendicular to each other (torsion angle = 90.1°). The atoms within the phenanthroline ligands are almost within its molecular plane. The thallium complex can be viewed as consisting of two equivalent Tl(phen)Cl units, each located in its own hemisphere of the coordination shell of Tl. In **4**, thallium is *cis*-coordinated by two Cl ligands similarly to the *cis*-dichlorobis(2,2′-bipyridyl)gallium(III) cation.[24] Four N atoms and two chloride ions form a distorted octahedral geometry around Tl. The

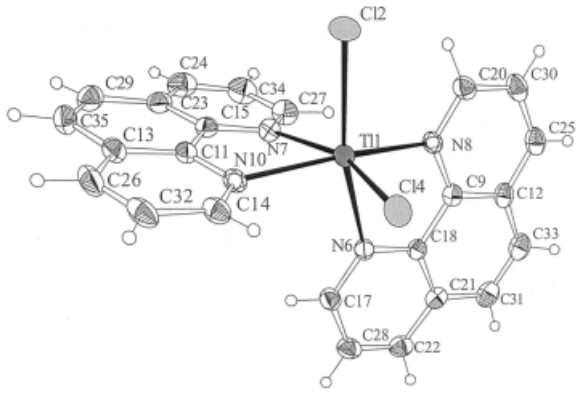

Figure 5. ORTEP view of the $[Tl(phen)_2Cl_2]^+$ cation found in the crystal structure of $[Tl(phen)_2Cl_2](ClO_4)$ (**4**); thermal ellipsoids are drawn at the 30% probability level; selected bond lengths [Å] and angles [°]: Tl(1)−N(8) 2.357(3), Tl(1)−N(7) 2.362(3), Tl(1)−N(10) 2.372(3), Tl(1)−N(6) 2.384(3), Tl(1)−Cl(4) 2.4655(9), Tl(1)−Cl(2) 2.4789(9); N(8)−Tl(1)−N(7) 96.81(10), N(7)−Tl(1)−N(10) 70.64(19), N(10)−Tl(1)−N(6) 98.95(10), N(8)−Tl(1)−Cl(4) 100.05(7), N(7)−Tl(1)−Cl(4) 160.29(8), N(10)−Tl(1)−Cl(2) 98.15(8), N(6)−Tl(1)−Cl(2) 159.35(7), Cl(4)−Tl(1)−Cl(2) 100.02(4)

mean Tl−N distance, 2.369(3) Å (2.357−2.384 Å), is similar to that in $[Tl(bipy)_3(DMSO)]^{3+}$ (2.356−2.372 Å), and the atomic arrangement is almost exactly the same as in the complex $[Tl(phen)Cl_3]$.[12] The mean Tl−Cl distance, 2.4722(9) Å (2.4655−2.4789 Å), is similar to the previously studied complex {$[Tl(phen)Cl_3]$: 2.467(3) Å}, but they are longer than those in tetrahedral $[TlCl_4]^-$ and shorter than those in $[TlCl_5(DMSO)]^{2-}$ [2.506(6)−2.636(6) Å][13] and $[TlCl_6]^{3-}$ (2.59 Å).[14]

Comparison of the Structures and Optical Properties

Apart from the previously discussed ^{205}Tl NMR chemical shift, the change in the actual oxidation state of the metal ions in the heterodinuclear compounds is also reflected by the bond lengths Tl−O and Tl−N. The bonds Tl−O [average 2.471(5) Å in **1**] and Tl−N [average 2.422(8) Å in **2**] are significantly longer than the corresponding distances in the mononuclear Tl^{III} complexes $[Tl(DMSO)_6]^{3+}$ [2.224(3) Å][11] and $[Tl(phen)_2Cl_2]^+$ [average 2.369(3) Å] (**4**). The increase in the Tl−O and Tl−N bond lengths in the studied Pt−Tl compounds is compatible with the decrease of the thallium oxidation state upon formation of the Pt−Tl bond. It confirms that the reaction of $[Tl^{III}(phen)_n]^{3+}$ (n = 1−2) with $[Pt^{II}(CN)_4]^{2-}$ to form heterodinuclear Pt−Tl metal−metal-bonded compounds $[(NC)_4Pt-Tl(phen)_n(solv)]^+$ and $[(NC)_5Pt-Tl(phen)_n(solv)]$ (n = 1,2) can be considered as an oxidative addition.

The optical properties of the dinuclear complexes $[(NC)_5Pt-Tl(CN)_n(aq)]^{n-}$ (n = 0−3) in aqueous solution are dominated by the metal−metal interaction. A very intensive electronic absorption band appears in the UV region, with the maximum in the range 238−259 nm (ε = $2.9-6.9\cdot10^4$ $L\cdot mol^{-1}\cdot cm^{-1}$) depending on the number of cyanide ligands in the compound.[3] The metal-to-metal charge-transfer band (MMCT) of the dinuclear complex $[(NC)_5Pt-Tl(solv)]$ in DMSO is found at 294 nm (ε = $2.1\cdot10^4$ $L\cdot mol^{-1}\cdot cm^{-1}$). Interestingly, the maximum MMCT band of $[(NC)_4Pt-Tl(solv)]^+$ in DMSO is found at 350 nm, which is a dramatic shift to the red compared to $[(NC)_5Pt-Tl(solv)]$. For all the dinuclear complexes studied, it seems that the maximum of the MMCT band is approximately proportional to the corresponding Pt−Tl spin-spin coupling constant. This phenomenon was also found for the dinuclear Pt−Tl cyano complexes. By comparing the electronic absorption spectra of $[(NC)_5Pt-Tl(phen)_2]$ and the parent complex $[Tl(phen)_3]^{3+}$, both in DMSO, the maximum for the former compound, at 274 nm (ε = $4.41\cdot10^4$ $L\cdot mol^{-1}\cdot cm^{-1}$), was assigned to the metal-to-metal charge transfer transition (MMCT). This corresponds to a shift by 15 nm to longer wavelength relative to the M−M transition in the complex $[(NC)_5Pt-Tl(H_2O)_5]$ in water. This shift is attributed to the change of thallium coordination (two phen ligands replace five water molecules). It can be concluded that there is no dramatic effect of the coordinated phenanthroline ligand on the MMCT transition.

^{195}Pt-^{205}Tl Spin-Spin Coupling Constants and ^{205}Tl NMR Chemical Shifts

Until now, ^{205}Tl NMR chemical shifts and Pt−Tl spin-spin coupling constants have been recorded for fifteen Pt−Tl heterodinuclear complexes in DMSO (cf. Supporting Information). Interestingly, the values of δ_{Tl} and $^1J(^{195}Pt-^{205}Tl)$ for all these complexes fall onto a straight line (Figure 6). This cannot be accidental, considering the very large intervals for both parameters, about 57000 Hz and 2140 ppm, respectively. As has been discussed previously,[20,21] the very large chemical shift variation is related to the oxidation state (large variation of the electron density) of the ^{205}Tl nucleus via the paramagnetic term of the Ramsey equation.[22] Also, the spin-spin coupling is related to the electron density: in the present case, the Pt−Tl coupling is transmitted via the s-electrons participating in the Pt−Tl bond.[23] The relation can be explained as follows: The Tl-coordinated ligands induce transfer of electrons from the Tl nucleus towards Pt. In this way, Tl becomes more deshielded, which leads to larger values of the Tl NMR chemical shift.

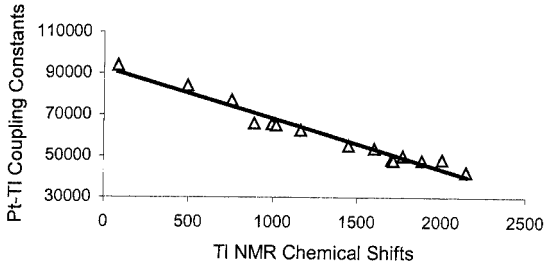

Figure 6. A correlation between the ^{205}Tl NMR chemical shifts (in ppm) and spin-spin coupling constants (in Hz) for all measured Pt−Tl bonded compounds in DMSO; the straight line follows the equation ^1J [Hz] = $-24.6\cdot\delta_{Tl}$ [ppm] + 92740

At the same time, the total electron density (and the density of the s electrons that contribute to the Fermi contact term)[23] of the Pt−Tl bond decreases, which leads to a decrease in the spin-spin coupling constant $^1J(^{195}Pt-^{205}Tl)$ and to a weakening of the Pt−Tl bond.

It would be interesting to compare the spin-spin coupling and chemical shifts of the two studied types of complexes $[(NC)_4Pt-Tl(phen)_n(solv)]^+$ and $[(NC)_5Pt-Tl(phen)_n(solv)]$ (n = 0, 1, and 2). A single cyanide ligand coordinated to the platinum atom in the axial position decreases the Pt−Tl coupling and increases the Tl chemical shifts dramatically. What could be the reason? It is probable that after the axial cyanide ligand has been coordinated, the electron-donating ability of the orbital d_{z^2} towards the Tl 6s orbital decreases, the electron density around Tl decreases and the Fermi contact term becomes small, so the real oxidation state increases. Meanwhile, the spin-spin coupling becomes small and the chemical shift increases.

It is also interesting to compare the Pt−Tl spin-spin coupling of the complex $[(NC)_5Pt-Tl]$ in two different solvents, water and DMSO. It is reasonable to consider that five molecules of H_2O or DMSO are coordinated to the thallium atom in the Pt−Tl dinuclear complex, in the same way as in the solid state.[6] In agreement with the stronger ability of DMSO to donate electron density to Tl^{III}, ^{205}Tl NMR chemical shift in solution of $[Tl(DMSO)_6]^{3+}$ (δ = 1886)[11] is smaller than that of $[Tl(H_2O)_6]^{3+}$ (δ = 2093).[19] Accordingly, the ^{205}Tl NMR chemical shift of the $[(NC)_5Pt-Tl]$ complex in DMSO should be smaller than for the same complex in aqueous solution. Also, the Pt−Tl coupling constant of $[(NC)_5Pt-Tl(DMSO)_5]$ should be larger than that of $[(NC)_5Pt-Tl(H_2O)_5]$. Surprisingly, both the ^{205}Tl NMR shifts and the coupling constants of the two complexes follow just the opposite trend, $[(NC)_5Pt-Tl(DMSO)_5]$ (δ = 887 and 65.9 kHz) and $[(NC)_5Pt-Tl(H_2O)_5]$ (δ = 786 and 71.1 kHz).

What could be the reason for this behaviour? One explanation is that the stronger electron donation from DMSO to the thallium atom would induce a partial transfer of electrons from Tl towards Pt, thus causing the observed trend for the chemical shifts and the spin-spin coupling constant Pt−Tl. An alternative explanation goes as follows: Very recently, theoretical calculations (DFT calculation considering relativistic effects)[23] led to a suggestion that short C≡N···H hydrogen bonds (N···H approximately 2.2 Å, see Scheme 2) are formed between the thallium-coordinated water molecules and the platinum-bonded cyanide ligands. This would lead to a strengthening of the Pt−Tl bond; indeed, the Pt−Tl distance would become quite short (Pt−Tl approximately 2.600 Å).[23] This type of hydrogen bond cannot form in DMSO solution; hence, it would be compatible with the (opposite to the expected) trend of the chemical shifts and the coupling constant.

Conclusions

Five novel Pt−Tl(phen) complexes in DMSO, $[(NC)_4Pt-Tl(solv)]^+$ (**1a**), $[(NC)_4Pt-Tl(phen)(solv)]^+$ (**2a**),

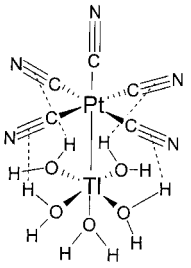

Scheme 2

$[(NC)_4Pt-Tl(phen)_2(solv)]^+$ (**3a**), $[(NC)_5Pt-Tl(phen)(solv)]$ (**2b**), and $[(NC)_5Pt-Tl(phen)_2(solv)]$ (**3b**) have been prepared and their formation shown by means of ^{205}Tl NMR. The very large ^{195}Pt-^{205}Tl spin-spin coupling constants, 94.0, 84.2, and 77.1 kHz for complex **1a**, **2a**, and **3a**, and 65.4 and 62.5 kHz for complex **2b** and **3b**, respectively, unambiguously demonstrate the presence of a direct metal−metal bond in the complexes. For the first time in Pt−Tl-bonded complexes, the species $[(NC)_4Pt-TlX]$ [where X = $(phen)_n(solv)$, n = 1 and 2] comply with the 16-electron rule, with respect to platinum. The results show that the complexes with 16 electrons are stable in solution, long enough for the study on the ^{205}Tl NMR time scale. Three solid compounds, $[(NC)_5Pt-Tl(phen)(DMSO)_3]$ (**2b**), $[(NC)_5Pt-Tl(phen)_2]$ (**3b**), and $[Tl(phen)_2Cl_2](ClO_4)$ (**4**), were crystallised from solution and their structures determined by X-ray diffraction. In compounds **2b** and **3b** unsupported metal−metal bonds are present. The Pt−Tl distances, 2.6296(3) and 2.6375(5) Å for **2b** and **3b**, respectively, are among the shortest reported separations between these two metals. The Pt−Tl force constants in the molecules **2b** and **3b**, 1.84 and 1.74 N/cm, respectively, calculated from Raman frequencies of the metal−metal stretching vibrations, are compatible with the intermetallic Pt−Tl separations; the values of the force constants are characteristic for a strong, single metal−metal bond. Attachment of phenanthroline to the thallium part of the dimetallic platinum−thallium(cyano) compounds resulted in a red shift of the metal-to-metal charge transfer band.

Experimental Section

Synthesis: The solid $[Tl(DMSO)_6](ClO_4)_3$ was prepared as described in a recent paper.[11] The complex $[(NC)_4Pt-Tl(solv)]^+$ (**1a**) was obtained by the reaction between solid compounds $[Tl(DMSO)_6](ClO_4)_3$ (49 mg, 0.05 mmol) and $K_2Pt(CN)_4$ (19 mg, 0.05 mmol), concentration 50 mM in 1 mL of DMSO. Upon addition of 1,10-phenanthroline to the solution of complex **1a**, the complexes **2a** and **3a** were prepared in solution. The reactions were monitored by ^{205}Tl NMR spectroscopy. The solid compound $[(NC)_5Pt-Tl(DMSO)_4](DMSO)$ was obtained as described previously.[4a] Two different routes were used to prepare compounds **2b** and **3b**: i) 49 mg of $[Tl(DMSO)_6](ClO_4)_3$ (0.05 mmol), 19 mg of $K_2Pt(CN)_4$ (0.05 mmol), and 9 mg or 18 mg of 1,10-phenanthroline (0.05 mmol or 0.1 mmol) for **2b** and **3b**, respectively, were added to 1 mL of DMSO in the presence of 50 mM NaCN. After stirring the

solutions for 5 h, compounds **2b** and **3b** formed in solution (see Scheme 1). ii) 46 mg (0.05 mmol) of solid $[(NC)_5Pt-Tl(DMSO)_4](DMSO)$ was dissolved in 1 mL of DMSO, then 11 mg (0.06 mmol) of 1,10-phenanthroline was added for compound **2b** and 20 mg (0.1 mmol) for compound **3b**. After stirring for half an hour, compounds **2b** and **3b** formed in solution. Crystals containing **2b** and **3b** suitable for X-ray analysis were crystallised by putting the resulting solutions inside a dark vacuum desiccator and slowly evaporating the solvent by degassing. Small round transparent white crystals formed at the bottom of the flask after several days. Raman spectra of the solid compounds **2b** and **3b** were recorded with a Renishaw System 1000 spectrometer equipped with a microscope (Leica DMLM). The abbreviations are: vs = very strong, s = strong, m = medium, w = weak. The band positions and assignments are as follows. **2b:** $\tilde{\nu}$ = 2995 m, 2915 s (CH_3 str.), 2184 s (axial C≡N str.), 2174 m, 2161 m (equatorial C≡N str.), 1206 w, 1102 m, 1002 m, 952 m (CH_3 bend), 712 s, 672 vs (CS str.), 452 s (TlO str.), 378 m, 308 m (CSC or OSC bend), 177 vs (Pt−Tl str.). $\tilde{\nu}$ (of coordinated phen) = 1621 w, 1603 w, 1588 w, 1516 m, 1446 m, 1412 vs, 1341 w, 1311 m, 1255 w, 1206 w, 1052 m, 862 w, 727 m, 552 s, 452 s 422 s, 402 m, 332 s 282 m, 257 w.

3b: $\tilde{\nu}$ = 2189 s (axial C≡N str.), 2178 m, 2160 m (equatorial C≡N str.), 172 vs (Pt−Tl str.). $\tilde{\nu}$ (of coordinated phen) = 1626 w, 1604 w, 1590 w, 1521 w, 1455 s, 1417 vs, 1344 w, 1306 s, 1252 w, 1207 w, 1139 w, 1103 m, 1060 m, 867 m, 728 s, 558 s, 463 s, 423 vs, 408 m, 332 s, 288 s, 261 m (for free phen: 1585 m, 1499 m, 1444 s, 1402 vs, 1341 m, 1291 s, 1094 m, 1032 s, 707 vs, 407 s, 242 m).

4: Colourless cubic crystals of compound **4** were obtained from a DMSO solution with the following composition: 50 mM $Tl(ClO_4)_3$, 100 mM 1,10-phenanthroline, and 200 mM Cl^- by slowly evaporating the solvent. Raman vibration bands of solid compound **4:** $\tilde{\nu}$ (of coordinated phen) = 1623 w, 1601 w, 1581 w, 1514 w, 1448 s, 1418 vs, 1336 w, 1306 s, 1248 w, 1198 w, 1144 w, 1102 m, 1052 m, 857 w, 726 s, 554 s, 437 s, 420 vs, 402 m, 280 m, 268 s. $\tilde{\nu}$ (of ClO_4^-) = 929 s.

^{205}Tl NMR Measurements: All ^{205}Tl NMR measurements were performed with a Bruker DMX500 spectrometer at a probe temperature of 25 (±0.5) °C. DMSO was used as solvent. The spectra were recorded at SF = 288.5 MHz; typical NMR parameters: flip angle about 30°; spectral window 86 kHz; pulse repetition time 0.5 s. The chemical shifts are reported in ppm toward higher frequency with respect to an external aqueous solution of $TlClO_4$ extrapolated to infinite dilution.

X-ray Crystal Structure Analysis: Suitable crystals of **2b**, **3b**, and **4** were selected under a polarizing microscope and mounted on a glass fibre. The data were collected with a Nonius Kappa CCD area detector, λ(Mo-K_α) = 0.71073 Å, using a graphite monochromator. Numerical absorption correction was applied.[15] The structures were solved by direct methods[16] and refined using full-matrix least squares on F^2 (SHELXL-97).[17] All the non-hydrogen atoms in compounds **2b**, **3b**, and **4** were refined with anisotropic displacement parameters. Hydrogen atoms were located at calculated positions and refined riding on their carrier atoms. In **3b**, one of the three non-coordinated DMSO molecules is disordered. Selected crystal data for compounds **2b**, **3b**, and **4** are listed in Table 1. CCDC-157362 (**2b**), -157363 (**3b**) and -157364 (**4**) contain the supplementary crystallographic data for this paper. These data can be obtained free of charge at www.ccdc.cam.ac.uk/conts/retrieving.html or from the Cambridge Crystallographic Data Centre, 12, Union Road, Cambridge CB2 1EZ, UK [Fax: (internat.) + 44-1223/336-033; E-mail: deposit@ccdc.cam.ac.uk].

Table 1. Selected crystal data for $[(NC)_5Pt-Tl(phen)(DMSO)_3]\cdot(DMSO)$ (**2b**), $[(NC)_5Pt-Tl(phen)_2]\cdot(DMSO)_3$ (**3b**), and $[Tl(phen)_2Cl_2](ClO_4)$ (**4**)

	2b	**3b**	**4**
Empirical formula	$C_{25}H_{32}N_7O_4S_4PtTl$	$C_{35}H_{34}N_9O_3S_3PtTl$	$C_{24}H_{16}Cl_3O_4N_4Tl$
Formula mass	1022.30	1124.38	735.16
Crystal system	monoclinic	monoclinic	triclinic
Space group	$P2_1/n$	$P2_1/c$	$P\bar{1}$
a [Å]	10.9206(2)	14.66400(10)	7.17280(10)
b [Å]	17.1743(3)	24.7240(3)	12.7524(2)
c [Å]	18.4541(3)	11.6700(2)	13.9575(16)
α [°]			107.1145(7)
β [°]	98.8160(6)	106.6090(4)	99.9867(7)
γ [°]			91.3280(19)
V [Å^3]	3420.20(10)	4054.46(9)	1197.94(3)
Z	4	4	2
Crystal size [mm]	0.12 × 0.25 × 0.29	0.13 × 0.12 × 0.26	0.13 × 0.13 × 0.25
$\rho_{calcd.}$ [g cm^{-3}]	1.728(1)	2.226(5)	2.936(5)
Temperature [K]	298(2)	298(2)	298(2)
μ (Mo-K_α) [mm^{-1}]	8.945	11.189	8.67
F(000)	1776	2520	981
θ range [°]	0.985−27.47	0.991−28.29	0.990−30.04
Limiting indices	$0 \le h \le 14$	$0 \le h \le 19$	$-8 \le h \le 10$
	$0 \le k \le 22$	$-32 \le k \le 32$	$-15 \le k \le 17$
	$-23 \le l \le 23$	$-15 \le l \le 14$	$-19 \le l \le 18$
N_{obs}, N_{par}	6849, 379	9992, 424	6938, 326
S (goodness of fit)	1.107	1.032	1.063
R_1,wR_2 [$I > 2\sigma(I)$][a]	0.0341, 0.0826	0.0569, 0.1311	0.0272, 0.0705
$\Delta\rho_{max}$, $\Delta\rho_{min.}$ [e/Å^3]	1.236, −1.489	1.192, −1.631	1.559, −1.468

[a] R values are defined as: $R(\text{int}) = \Sigma|F_o^2 - F_o^2(\text{mean})|/\Sigma[F_o^2]$, $S = \{\Sigma[w(F_o^2 - F_c^2)^2]/(n-p)\}^{1/2}$. $R_1 = \Sigma||F_o| - |F_c||/\Sigma|F_o|$, $wR_2 = \{\Sigma[w(F_o^2 - F_c^2)^2]/\Sigma[w(F_o^2)^2]\}^{1/2}$, $w = 1/[\sigma^2 F_o^2 + (ap)^2 + bp]$, $p = (1/3)\max(0,F_o^2) + (2/3)F_o^2$.

Supporting Information: See footnote on the first page of this article. Table of NMR parameters for Pt−Tl compounds and related platinum and thallium species in solution.

Acknowledgments

The authors are grateful to The Swedish Natural Science Research Council (NFR) for providing funds for purchasing the diffractometer and for the continuous financial support for the project. The Swedish Institute fellowship for the stay of G.-B. M. in Stockholm is gratefully acknowledged.

[1] [1a] T. Yamaguchi, F. Yamazaki, T. Ito, *J. Am. Chem. Soc.* **1999**, *121*, 7405−7406. (and references therein). [1b] J. K. Nagle, A. L. Balch, M. M. Olmstead, *J. Am. Chem. Soc.* **1988**, *110*, 319−321.

[2] [2a] O. Ezomo, M. P. Mingos, I. D. Williams, *J. Chem. Soc., Chem. Commun.* **1987**, 924−925. [2b] L.-J. Hao, J. J. Vittal, R. J. Puddephatt, *Inorg. Chem.* **1996**, *35*, 269−270. [2c] L.-J. Hao, J. Xiao, J. J. Vittal, R. J. Puddephatt, L. Manojlovic-Muir, K. W. Muir, A. A. Torabi, *Inorg. Chem.* **1996**, *35*, 658−666. [2d] L.-J. Hao, J. J. Vittal, R. J. Puddephatt, *Organometallics* **1996**, *15*, 3115. [2e] R. Uson, J. Fornies, M. Tomas, R. Garde, P. Alonso, *J. Am. Chem. Soc.* **1995**, *117*, 1837−1838. [2f] A. Balch, S. Rowley, *J. Am. Chem. Soc.* **1990**, *112*, 6139−6140. [2g] O. Renn, B. Lippert, *Inorg. Chim. Acta* **1993**, *208*, 219−223. [2h] I. Ara, J. R. Berenguer, J. Fornies, J. Gomez, E. Lalinde, R. I. Merino, *Inorg. Chem.* **1997**, *36*, 6461−6464. [2i] R. Uson, J. Fornius, M. Tomas, R. Garde, *Inorg. Chem.* **1997**, *36*, 1383−1387. [2j] V. J. Catalano, B. L. Bennett, S. Muratidis, B. C. Noll, *J. Am. Chem. Soc.* **2001**, *123*, 173, and references therein.

[3] [3a] K. E. Berg, J. Glaser, M. C. Read, I. Tóth, *J. Am. Chem. Soc.* **1995**, *117*, 7550. [3b] M. Maliarik, K. Berg, J. Glaser, M. Sandström, I. Tóth, *Inorg. Chem.* **1998**, *37*, 2910. [3c] M. Maliarik, J. Glaser, I. Tóth, M. W. da Silva, L. Zekany, *Eur. J. Inorg. Chem.* **1998**, 565. [3d] J. Glaser, *Advances in Inorganic Chemistry*, Academic Press, Inc., London, **1995**, vol. 43.

[4] [4a] G.-B. Ma, M. Kritikos, J. Glaser, *Eur. J. Inorg. Chem.* **2001**, 1311. [4b] G.-B. Ma, M. Kritikos, M. Maliarik, J. Glaser, *Inorg. Chem*, submitted. [4c] Unpublished results from this laboratory.

[5] Md. K. Nazeeruddin, P. Liska, J. Moser, N. Vlachopoulos, M. Grätzel, *Helv. Chim. Acta* **1990**, *73*, 1788.

[6] [6a] F. Jalilehvand, J. Glaser, M. Maliarik, J. Mink, I. Persson, P. Persson, M. Sandström, I. Tóth, *Inorg. Chem.*, **2001**, *40*, 3889−3899. [6b] F. Jalilehvand, PhD Thesis, Royal Institute of Technology (KTH), Stockholm, Sweden, **2000**.

[7] [7a] P. Laszlo, *NMR of Newly Accessible Nuclei*, Academic Press, New York, **1983**, vol. 2. [7b] J. Mason, *Multinuclear NMR*, Plenum Press, New York, **1987**.

[8] Force constants in N/cm were calculated from $k = (5.889 \cdot 10^{-7}) \cdot \tilde{\nu}^2 \cdot \mu$, where $\tilde{\nu}$ is wavenumber in cm^{-1} and $\mu = M_{Pt} \cdot M_{Tl}/(M_{Pt} + M_{Tl})$, with atomic masses of the metals in Daltons.

[9] Recently completed calculations of the metal−metal stretching force constants in the complexes $[(NC)_5Pt-Tl(CN)_n]^{n-}$ (n = 0−3) show that in a full model, taking into account all vibrational modes (both metal−metal and metal−ligands), about 92% is attributed to purely diatomic Pt−Tl stretch (see ref.[6a]).

[10] [10a] F. A. Cotton, R. A. Walton, *Multiple Bonds Between Metal Atoms*, 2nd ed., Clarendon Press, Oxford, **1993**. [10b] D. F. Shriver, C. B. Cooper, *Vibrational Spectroscopy of Metal-Metal Bonded Transition Metal Compouunds*, Heyden, London, **1980**, vol. 6, pp. 127−157.

[11] G.-B. Ma, A. Molla-Abbassi, M. Kritikos, A. Ilyukhin, F. Jalilehvand, V. Kessler, M. Skripkin, M. Sandström, J. Glaser, J. Näslund, I. Persson, *Inorg. Chem.* **2001**, *40*, 6432−6438.

[12] W. J. Baxter, G. Gafner, *Inorg. Chem.* **1972**, *11*, 176−178.

[13] B. D. James, M. B. Millikan, M. F. Mackay, *Inorg. Chim. Acta* **1983**, *77*, L251.

[14] [14a] J. Blixt, J. Glaser, I. Persson, P. Mink, M. Sandström, *J. Am. Chem. Soc.* **1995**, *117*, 5089−5104. [14b] J. Glaser, *Acta Chem. Scand., Ser. A* **1982**, *36*, 451.

[15] W. Herrendorf, H. Bärnighausen, *HABITUS, A program for numerical absorption correction*, University of Karlsruhe, **1993**.

[16] G. M. Sheldrick, *Acta Crystallogr., Sect. A* **1990**, *46*, 467−473.

[17] G. M. Sheldrick, *SHELXL97 Program for the Refinement of Crystal Structures*, University of Göttingen, Germany, **1997**.

[18] M. N. Memering, L. H. Jones, J. C. Bailar, *Inorg. Chem.* **1973**, *12*, 2793.

[19] I. Bányai, J. Glaser, *J. Am. Chem. Soc.* **1989**, *111*, 3186.

[20] M. Buhl, M. HÅkansson, A. H. Mahmoudkhani, L. Öhrström, *Organometallics.* **2000**, *19*, 5589.

[21] M. C. Read, J. Glaser, M. Sandström, *J. Chem. Soc., Dalton Trans.* **1992**, 233.

[22] [22a] N. F. Ramsey, *Phys. Rev.* **1950**, *78*, 699. [22b] J. Mason, *Chem. Rev.* **1987**, *87*, 1299.

[23] [23a] J. Autschbach, T. J. Ziegler, *J. Am. Chem. Soc.* **2001**, *123*, 5320. [23b] N. Kaltsoyannis, *J. Chem. Soc., Dalton Trans.* **1997**, 1. [23c] M. R. Russo, N. Kaltsoyannis, *Inorg. Chim. Acta* **2001**, *312*, 221−225.

[24] R. Restivo, G. J. Palenik, *J. Chem. Soc., Chem. Commun.* **1969**, 867.

Received July 2, 2001
[I01245]